

# Energy Efficiency Improvement in Biomass Cookstoves through Inert Material Integration: Experimental Evaluation Considering Pot Size and Operating Phases

Drissa Ouedraogo<sup>1,2,3\*</sup>, Gaël Lassina Sawadogo<sup>1,2,3</sup>, Boureima Kabore<sup>3,4</sup>, Adama Sana<sup>3,4</sup>, Serge Wendsida Igo<sup>3,5</sup>

<sup>1</sup>Laboratory of Materials, Heliophysics and the Environment (La.M.H.E.), Nazi BONI University, Bobo-Dioulasso, Burkina Faso

<sup>2</sup>Laboratory of Chemistry and Renewable Energies (LaCER), Nazi BONI University, Bobo-Dioulasso, Burkina Faso

<sup>3</sup>Laboratory of Renewable Thermal Energies (LETRE), Joseph KI-ZERBO University, Ouagadougou, Burkina Faso

<sup>4</sup>Laboratory of Research in Energy and Space Meteorology, Norbert ZONGO University, Koudougou, Burkina Faso

<sup>5</sup>Department of Energy, Institute of Research in Applied Sciences and Technologies (IRSAT/CNRST), Ouagadougou, Burkina Faso

Email: \*ouedraogodri2016@gmail.com

**How to cite this paper:** Ouedraogo, D., Sawadogo, G.L., Kabore, B., Sana, A. and Igo, S.W. (2026) Energy Efficiency Improvement in Biomass Cookstoves through Inert Material Integration: Experimental Evaluation Considering Pot Size and Operating Phases. *Advances in Materials Physics and Chemistry*, **16**, 213-233.

<https://doi.org/10.4236/ampc.2026.166011>

**Received:** April 19, 2026

**Accepted:** May 29, 2026

**Published:** June 2, 2026

Copyright © 2026 by author(s) and Scientific Research Publishing Inc.

This work is licensed under the Creative Commons Attribution International License (CC BY 4.0).

<http://creativecommons.org/licenses/by/4.0/>



Open Access

## Abstract

This study follows on from our previous work on the comparative analysis of the thermal performance of improved cookstoves based on pot size. It focuses on the experimental evaluation of the effect of integrating inert materials (granite) into an improved charcoal-fired cookstove. The tests were conducted according to the Water Boiling Test (WBT) protocol in three phases: cold start, hot start, and simmering, using pots of sizes 2 and 3. The parameters analyzed were specific fuel consumption, thermal efficiency, fire intensity, specific boiling time, and water temperature evolution. The results show that the addition of inert materials improves the overall performance of the cookstove. These materials act as heat storage and release agents, which reduces heat loss and optimizes fuel use, particularly during the simmering phase. For pot 2, the results indicate a significant reduction in specific fuel consumption (up to 0.069 kg/L) as well as good efficiency during the simmering phase ( $\approx 38\%$ ), although boiling times are sometimes longer. For pot size 3, performance is generally superior, with efficiencies reaching over 40% during hot start-up and nearly 48% during simmering, as well as shorter boiling times. The study shows that inert materials play an important role in accumulating and releasing heat,

promoting better thermal stability of the firebox and reducing energy losses, particularly during simmering. Pot size 3 exhibits the shortest overall boiling times, reflecting a better geometric fit with the firebox. These results confirm that the integration of inert materials is an effective strategy for improving charcoal cooking fires.

### Keywords

Improved Hearth, Charcoal, Inert Material, Granite, Thermal Efficiency, Specific Consumption, Cooking Pot

---

## 1. Introduction

Improving the thermal and energy performance of cooking stoves is a major scientific and socio-technical challenge in developing countries, where solid biomass remains the primary source of domestic energy. Traditional stoves generally have low thermal efficiencies, often less than 20%, accompanied by significant losses through convection, conduction, and radiation, which increases fuel consumption and puts further pressure on forest resources [1]-[3]. Several studies have shown that improved stoves allow for a significant reduction in biomass consumption thanks to better control of heat transfer between the combustion zone and the cooking vessel [4]-[6]. The performance achieved depends heavily on the stove's geometry, the quality of combustion, the height of the combustion chamber, and the size of the pot used [7]-[9]. Following on from this issue, our previous study, which focused on the comparative analysis of the thermal performance of improved cookstoves using charcoal and wood as a function of pot size, showed that the diameter of the container directly influences thermal efficiency, specific consumption, and specific boiling time [10]. The results showed that a better geometric fit between the pot and the cookstove promotes more efficient heat transfer and reduces energy losses [11].

This work is a direct continuation of that initial study. It aims to further the analysis by incorporating inert materials (granite) into the charcoal to assess their influence on the thermal performance of improved cookstoves using size 2 and 3 pots. This approach is based on the hypothesis that inert materials, thanks to their high thermal inertia, can store some of the energy released by combustion and gradually release it back into the cooking vessel, thus improving the overall efficiency of the system [12]. The integration of materials with high thermal capacity into cooking stoves is currently a promising energy optimization strategy. Several authors have shown that the use of refractory or mineral materials improves the thermal stability of stoves, particularly during simmering phases, where energy requirements are lower but prolonged [13]-[15]. Furthermore, the performance of improved cookstoves remains highly dependent on the operating conditions. The cold start, hot start, and simmer phases exhibit distinct heat transfer mecha-

nisms, which can be accurately analyzed using the standardized Water Boiling Test (WBT) protocol [1] [9]. This methodology allows for the quantification of key thermal and energy indicators such as efficiency, specific consumption, power, and boiling time.

The objective of this study is therefore to experimentally evaluate the effect of adding inert materials on the thermal performance of an improved charcoal-fired cookstove, taking into account the size of the pot and the different phases of the test. Through this approach, this work aims to propose more energy-efficient cooking solutions, better suited to local domestic uses and contributing to the reduction of charcoal consumption.

## 2. Materials and Methods

### 2.1. Materials

The experiments were conducted using the following equipment:

- ✓ An improved cooking stove, designed to operate on charcoal and adapted for thermal performance testing;
- ✓ Charcoal, used as the primary fuel for the different phases of the test;
- ✓ Inert materials such as granite, integrated into the combustion chamber to improve thermal inertia and the gradual release of heat;
- ✓ Two metal pots, sizes 2 and 3, used for the comparative evaluation of the stove's thermo-energy performance;
- ✓ Water, used as the test fluid in accordance with the Water Boiling Test (WBT) protocol;
- ✓ An infrared thermometer with a flexible probe, used to measure the water temperature;
- ✓ A stopwatch, allowing for the precise measurement of boiling time and the different cooking phases;
- ✓ A precision electronic balance, used to determine the initial and final mass of the charcoal in order to evaluate specific consumption;
- ✓ A metal tray, used to hold the coal and inert materials during testing;
- ✓ A device for measuring ambient conditions, for recording the outside temperature during testing;
- ✓ The size 2 and 3 cooking pots, commonly used in domestic culinary practices in Burkina Faso, have respective diameters of 24 cm and 27 cm, corresponding to nominal capacities of 3 L and 4 L [16];
- ✓ For test 1, we used 0.45 kg of charcoal and 0.45 kg of granite. For test 2, we used 0.45 kg of charcoal and 0.3 kg of granite.

**Figure 1** shows the digital thermometer, the digital scale, and the wooden mold.

**Figure 2** shows the coal associated with inert material (granite).

We used SolidWorks, a computer-aided design (CAD) software, to represent the physical model of our fireplace (see **Figure 3**). It allows us to:

- ✓ Design parts in 2D or 3D;

- ✓ Create assemblies;
- ✓ Generate technical drawings.



**Figure 1.** a) Digital thermometer, b) Digital scale, c) Wooden mold measuring  $30 \times 14 \text{ cm} \times 10 \text{ cm}$ .



**Figure 2.** Coal associated with inert material (granite).

**Figure 3** shows the 3D model of the improved fireplace.

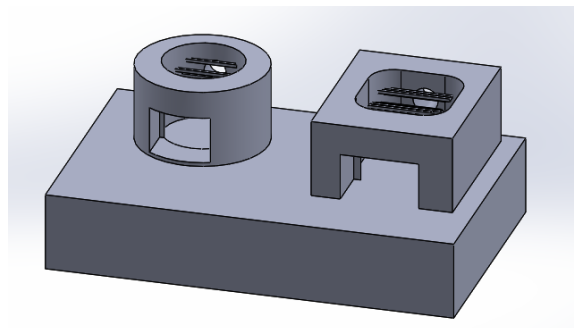


**Figure 3.** 3D physical model of the improved fireplace.

**Figure 4** presents the annotated diagram of the improved fireplace with the different views.

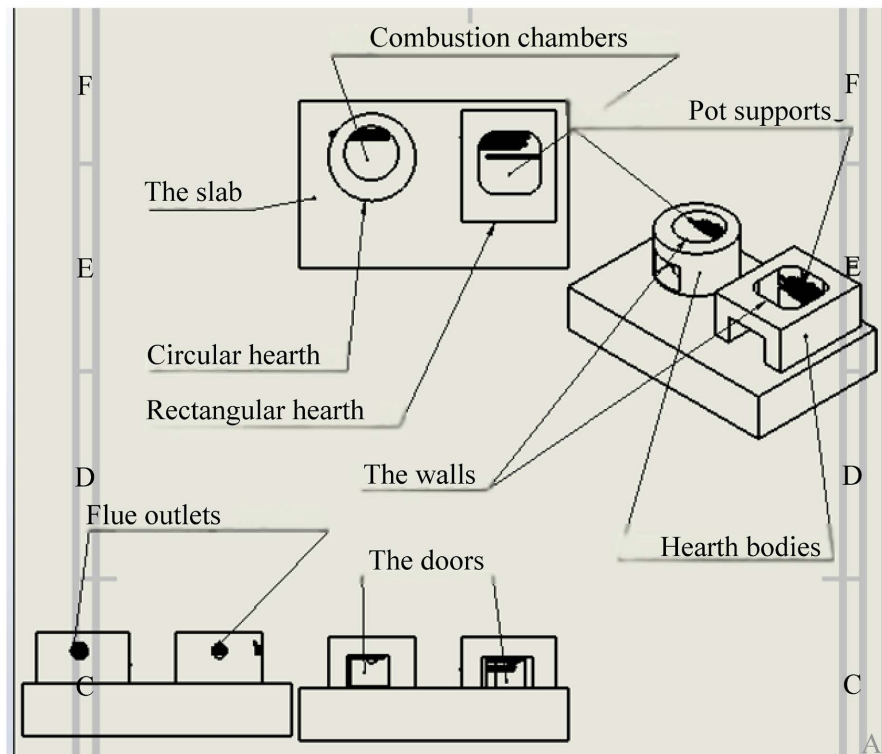


**Figure 4.** Annotated diagrams of the improved two-chamber combustion chamber fire-place designed with SolidWorks.

#### ❖ Experimentation process

To evaluate the thermal performance of the improved cookstoves, we established a rigorous protocol for measuring internal and external temperatures, as well as other parameters. This protocol aims to ensure the reliability and reproducibility of the results by controlling the parameters influencing combustion and heat transfer. To achieve this, we should:

- ✓ clean the cookstoves and ensure they are at room temperature;
- ✓ measure the room temperature;
- ✓ weigh the required quantity of well-dried charcoal;
- ✓ weigh a certain quantity of pebbles;
- ✓ weigh and record the mass of the empty pot;
- ✓ weigh the pot containing water;
- ✓ measure the temperature of the water in the pot;
- ✓ light the fire with kindling and ensure the charcoal is burning properly before placing the pot on it, then start the timer and note the starting time;
- ✓ Monitor the water until it boils (99.5°C or even 100°C), then note the time required;
- ✓ Weigh and note the mass of the pot containing the water, the remaining charcoal, and the ashes;
- ✓ Extinguish the fire and repeat. The second test is similar to the first;
- ✓ Add the required amount of charcoal again;

- ✓ Add the same amount of water as before, at room temperature, weigh it, and note the weight;
- ✓ Light the fire as usual, ensure it burns properly, then place the pot on the charcoal and start the timer;
- ✓ Stop the timer and note the time elapsed when the water reaches boiling point;
- ✓ Weigh the pot containing the water and the remaining charcoal. At this point, the weight of the ash is considered the high-power setting with a cold start;
- ✓ Take the water temperature and reset the timer with the pot containing the hot water;
- ✓ Simmer the water at a temperature close to boiling ( $T_{éb}-3^{\circ}\text{C}$ ) for 45 minutes, then turn off the heat. Maintain the temperature so that it does not drop more than  $6^{\circ}\text{C}$  below the boiling point. If it drops too low, the test is invalid;
- ✓ Weigh the pot containing the hot water, the charcoal, and the ash. After weighing these fuels, the pots, and the water, light the fire using kindling, ensuring that the fuel is burning properly before placing the pot on it. Start the timer, and record the water temperature every five minutes until boiling is reached. **Figure 5** shows the experimental setup with the charcoal combined with an inert material.



**Figure 5.** Experimental setup with charcoal combined with an inert material.

## 2.2. Methods

To assess the energy performance of our home, we determine various parameters such as the specific boiling time (SBT), specific consumption (SC), boiling efficiency, etc. These parameters are defined as follows:

### 2.2.1. The Specific Boiling Time

The specific boiling time corresponds to the time elapsed between the placement of the pot on the hob and the water reaching its boiling point. It is given by Equation (1) [17].

$$TES = \frac{TEB}{(M_s - M_{es})} \times \frac{100}{(100 - T_i)} \quad (1)$$

### 2.2.2. Thermal Efficiency at Boiling

The boiling point efficiency, denoted  $\eta_{ebb}$  corresponds to the ratio between the

energy received to bring the water to boiling and the energy consumption of the fuel [18]. The efficiency (%) is given by Equation (2) [19].

$$\eta_{\text{ébl}} = \frac{C_{pe} M_i (T_{\text{ébl}} - T_i) + L_v M_{ev}^{\text{ébl}}}{PCI \times M_b^{\text{ébl}}} \quad (2)$$

### 2.2.3. Specific Consumption (CS)

It represents the quantity of fuel required to obtain one unit of production [20]. It is expressed in kilograms per litre (kg/L) and is given by the following relation (3).

$$CS = \frac{75}{(100 - T_i)} \times \frac{M_{\text{cons}}}{M_{\text{res}}} \quad (3)$$

### 2.2.4. The Thermal Power of the Fireplace (P)

The fire power ( $P$ ) corresponds to the ratio between the thermal energy released by the combustion of the fuel (wood, charcoal, etc.) and the time required for this combustion. It is expressed in watts (W) for each phase of the test [21]. It is given by the following relationship (4):

$$P = \frac{M_{\text{cons}} \times PCI}{60(t_f - t_i)} \quad (4)$$

### 2.2.5. Combustion Rate

This is a quantity that measures the rate of fuel consumption during the boiling of water. It is the ratio of the dry fuel consumed to the time taken for the test. This relationship is given by Equation (5) [22].

$$\tau_c = \frac{M_{\text{cons}}}{(t_f - t_i)} \quad (5)$$

## 3. Results and Discussion

### 3.1. Results Following the Charcoal Production Accompanied by Inert Materials for the Size Pot

**Table 1** shows the meteorological conditions for carrying out the cooking hearth tests.

**Table 1.** Meteorological conditions for conducting the tests of the cooking pot hearth.

External conditions	Cold start		Hot start		Simmering	
Ambient temperature (°C)	31	25.2	30.2	28	29	30.1

#### 3.1.1. Performance Indicators for the Cooking Pot 2

**Figure 6** represents the specific consumption with charcoal associated with inert materials by the size 2 pot.

**Figure 6** shows that, regardless of the phase considered, the specific consumption of test 1 is always lower than that of test 2. First, we observe values of  $0.069 \pm 0.003$  kg/L versus  $0.072 \pm 0.003$  kg/L for the cold start. Then, we have  $0.12 \pm 0.003$

kg/L versus  $0.14 \pm 0.004$  kg/L for the hot start. Finally, we note  $0.09 \pm 0.003$  kg/L versus  $0.13 \pm 0.004$  kg/L for the simmering phase. Among the three phases, the lowest value is  $0.066$  kg/L for test 1 at the cold start, while the highest value is  $0.143$  kg/L for test 2 at the hot start. This demonstrates better coal economy in test 1 and greater heat losses in test 2. The decrease in specific consumption is explained by the presence of a significant amount of inert material in the firebox. As these materials heat up, they absorb heat and then transfer it to the pot by conduction. Thus, heat losses are reduced because the heat is transferred directly to the bottom of the pot, limiting losses by convection with the ambient air and by radiation through the firebox walls. The mixture of charcoal with these materials therefore contributes to better fuel economy. However, the high values observed during the hot start in both tests indicate the influence of wind during these experimental periods. **Figure 7** shows the thermal efficiency obtained with charcoal combined with inert materials in the size 2 pot.

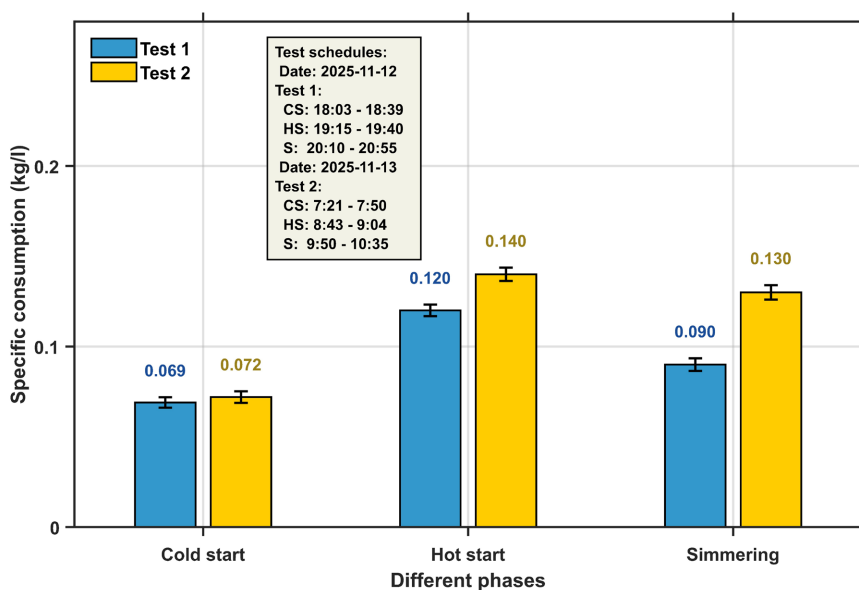


**Figure 6.** Comparison of the two trials of the specific consumption of the size 2 pot.

**Figure 7** shows the thermal efficiency obtained with the size 2 pot. Test 2 shows a slightly higher thermal efficiency than test 1 during the cold start phase ( $43.68\% \pm 0.52\%$  vs.  $33.86\% \pm 0.49\%$ ) and the hot start phase ( $29.87\% \pm 0.16\%$  vs.  $23.95\% \pm 0.18\%$ ). However, during the simmering phase, test 1 shows a significantly higher efficiency ( $38.38\% \pm 0.33\%$ ) than test 2 ( $12.7\% \pm 0.13\%$ ). These differences reflect a difference in heat transfer conditions between tests, with heat losses, particularly by convection to ambient air and by radiation, depending on the operating phase. The low yield of test 2 during simmering is characterized by low-intensity combustion of the charcoal, thus limiting the available heat output. This results in a prolonged boiling time. **Figure 8** shows the specific boiling time obtained with charcoal mixed with inert materials in the firebox of size 2 pot.

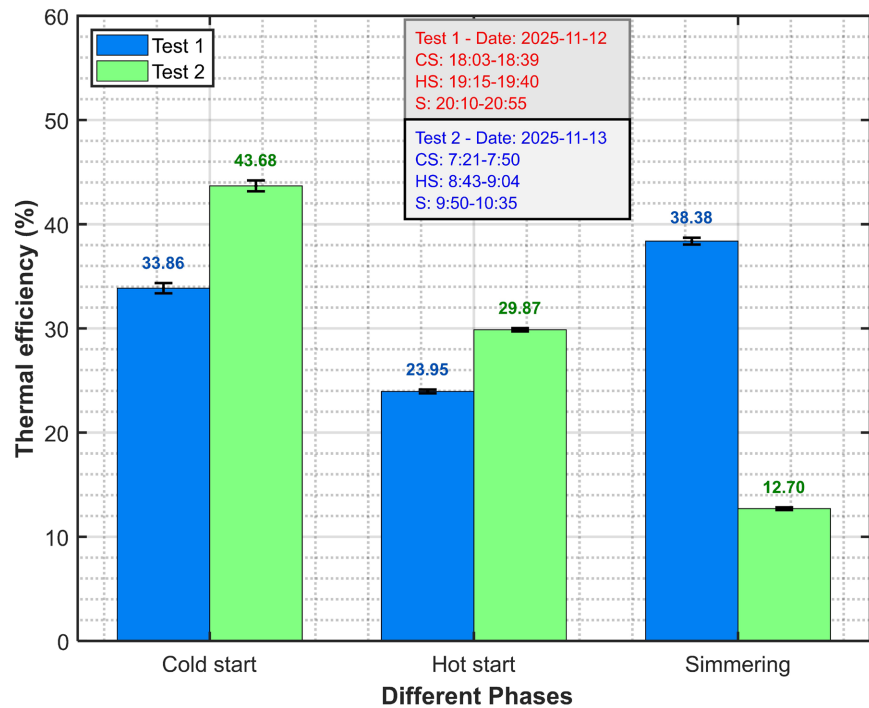


**Figure 7.** Boiling thermal efficiency per phase of the hearth of a size 2 pot of charcoal plus inert material.

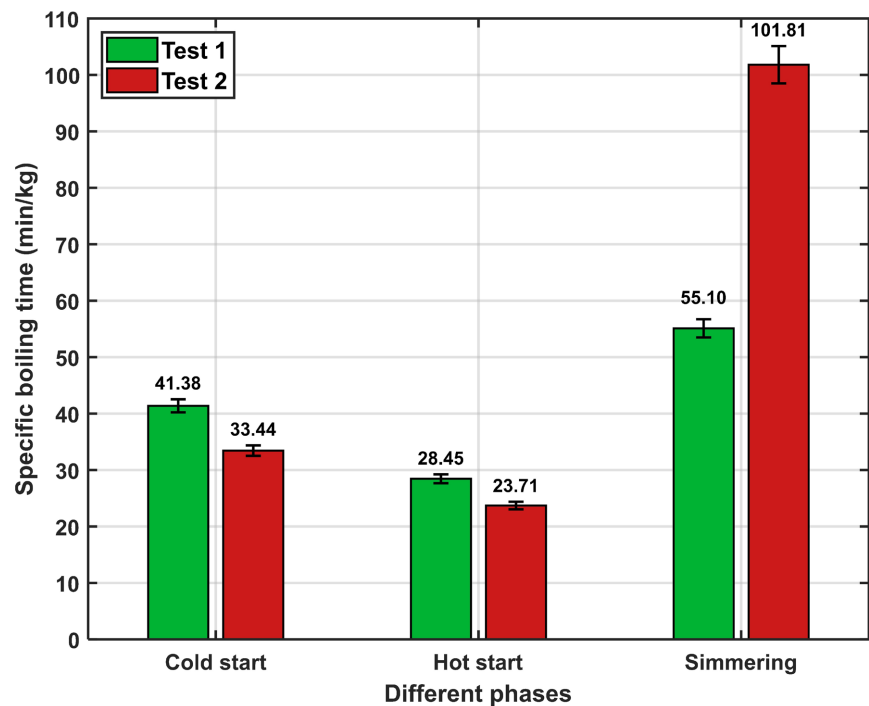


**Figure 8.** Specific Boiling Time of charcoal plus inert material in a size 2 pot.

**Figure 8** shows the evolution of the Specific Boiling Time for the two tests considered. It appears that, under high power conditions, test 1 exhibits a slightly longer specific boiling time than test 2, while the trend is reversed under low

power conditions. For cold start, we have  $41.38 \pm 1.164$  L/min versus  $33.44 \pm 0.933$  min/L. For hot start, we have  $28.45 \pm 0.795$  min/L versus  $23.71 \pm 0.671$  min/L. Finally, during the simmering phase, we have  $55.10 \pm 1.613$  min/L versus  $101.81 \pm 3.306$  min/L. This translates to good heat transfer in test 2, with a reduced heating time. In summary, we observe that test 1 has lower specific energy consumption, with higher efficiency during the simmering phase, but a longer specific boiling time than test 2. The last test (test 2) shows higher energy consumption with better efficiency during the start-up phase and shorter boiling times. In conclusion, the burner used in test 1 is more energy-efficient, while the one in test 2 has faster heating and better efficiency at the beginning of cooking.

### 3.1.2. Evolution of Thermal Efficiency as a Function of Fire Power for the Size 2 Pot

Figure 9 shows the thermal efficiency as a function of power.

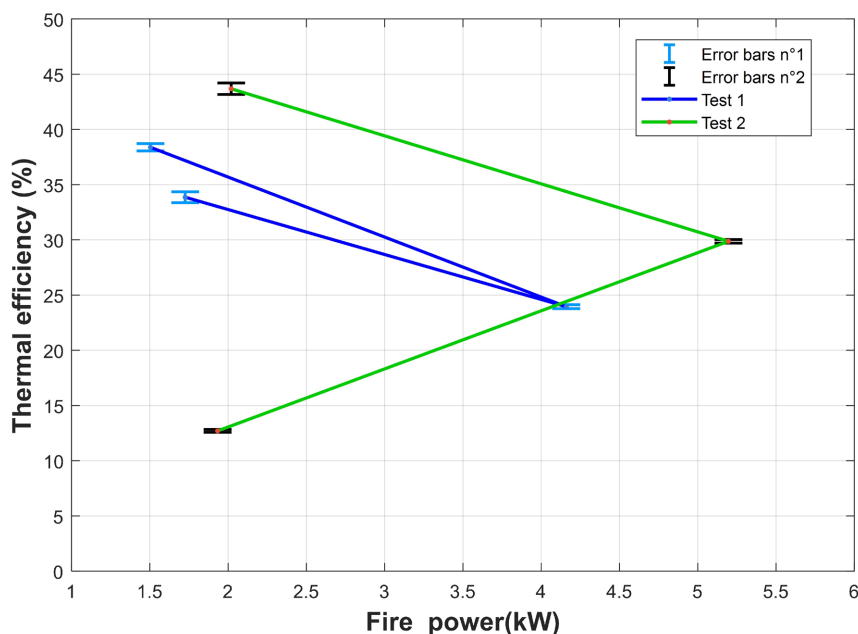


Figure 9. Thermal efficiency as a function of the fire power of the size 2 pot (coal + material (granite)).

In Figure 9, the power outputs during cold start-up are relatively low, with values close to 1.726 kW and 2.02 kW, corresponding to relatively high efficiencies of  $33.86 \pm 0.49\%$  and  $43.68 \pm 0.52\%$ , respectively. This observation is explained by the fact that a large portion of the thermal energy produced is used for heating the water, as heat losses are still low at the beginning of the process. In contrast, during hot start-up, the power outputs reach 4.160 kW and 5.196 kW, respectively, with lower efficiencies of approximately  $29.87 \pm 0.16\%$  and  $38.38 \pm 0.33\%$ . Increasing the fire leads to increased energy losses through convection with the ambient air and radiation into the environment. During the simmering phase, the power outputs become very low, with values of 1.504 kW and 1.933 kW. The as-

sociated efficiencies are  $38.38 \pm 0.33\%$  for test 1 and  $12.7 \pm 0.13\%$  for test 2, respectively. The low efficiency observed during test 2 is explained by insufficient combustion, linked to flame instability under the pot.

### 3.1.3. Evolution of Water Temperature over Time

**Figure 10** shows the different curves corresponding to each phase of the TEE, as well as the ambient air temperature.

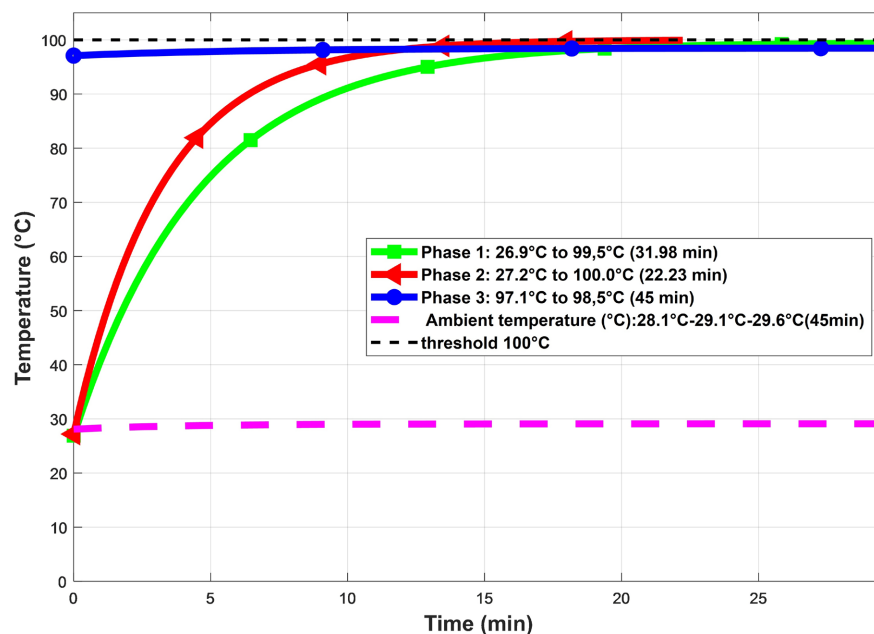


**Figure 10.** Evolution of water temperature over time for pot size 2.

The results show that the time required to reach boiling point decreases, from 31.98 minutes in phase 1 (cold start) to 22.23 minutes in phase 2 (hot start). This reduction is due to a rise in the temperature of the already hot burner, which promotes heat transfer to the pot. Phase 3 (simmering) maintains an average temperature of 98.5°C, close to boiling, for 45 minutes, indicating that the burner can maintain a stable temperature suitable for cooking.

## 3.2. Results Following the Charcoal Production Accompanied by Inert Materials for the Size 3 Pot

The results obtained highlight a significant variation in combustion rate during the different phases of use of the improved cookstoves, reflecting thermal dynamics consistent with the mechanisms of heat transfer and solid fuel oxidation. The cold start phase exhibits the highest average combustion rate (17.22 g/min), which is explained by the high energy demand required to raise the initial temperature of the system (cooker-fuel-container). This observation is consistent with the work of Berrueta *et al.* (2008), who show that heat losses are greatest at the beginning of combustion due to the lack of thermal equilibrium and incomplete combustion [20]. The decrease observed during the hot start (11.79 g/min) reflects an

energy efficiency linked to the establishment of more stable combustion conditions. At this stage, the high temperature promotes better fuel pyrolysis and more complete oxidation of the combustible gases, particularly the specific consumption. Similar trends were reported by Bailis *et al.* (2007) and Jetter *et al.* (2012) emphasize that improved stoves reach their optimal performance when draft and temperature conditions are stabilized [22] [23]. The simmering phase is characterized by a significant drop in the combustion rate (4.05 g/min), reflecting a balance between energy input and reduced heat requirements. This low consumption is indicative of operation in a quasi-steady state, where losses are minimized and overall efficiency maximized. This behavior is consistent with the observations of Kshirsagar and Kalamkar (2014), who showed that high-performance stoves allow for a significant reduction in fuel consumption during the slow cooking phase [24]. Furthermore, the variability observed between tests, particularly during the cold start phase, highlights the influence of operating conditions (ignition, fuel distribution, environmental conditions). This experimental variability is also reported by Okafor and Unachukwu (2012), who emphasize the need to standardize experimental protocols to improve the reproducibility of stove performance tests [18]. Overall, the gradual decrease in combustion rate over the three phases (17.22 → 11.79 → 4.05 g/min) confirms the ability of the improved stoves to adapt their operation to actual energy needs. This behavior reflects improved energy efficiency compared to traditional stoves, as demonstrated by Mekonnen *et al.* (2022), with substantial reductions in biomass consumption and associated emissions [25]. **Table 2** shows the weather conditions during the tests carried out with pot fireplace no. 3. **Table 3** shows the evolution of the combustion speed of improved stoves according to the phases of use (cold start, hot start and simmering phase).

**Table 2.** Weather conditions during tests carried out with the No. 3 pot firebox.

External conditions	Cold start		Hot start		Simmering	
Ambient temperatures (°C)	25.7	24.2	25.2	26	25	27

**Table 3.** Evolution of the combustion speed of improved stoves according to the phases of use (cold start, hot start and simmering phase).

	Phase 1 (cold start)			Phase 2 (hot start)			3rd phase (simmering)		
	Test 1	Test 2	moy	Test 1	Test 2	moy	Tes 1	Test 2	moy
Combustion rate (g/min)	22.44	12	17.22	9.56	14.02	11.79	4.77	3.33	4.05

### 3.2.1. Performance Indicators for a Size 3 Pot

We present in **Figure 11** the consumption obtained with charcoal associated with inert materials by the size n°3 pot only.

**Figure 11** shows the specific fuel consumption for tests 1 and 2 during the different operating phases. During a cold start, the specific fuel consumptions are  $0.162 \pm 0.002$  kg/L and  $0.101 \pm 0.002$  kg/L for tests 1 and 2, respectively. Test 1

shows a significantly higher consumption, indicating initial ignition difficulties due to the presence of a large quantity of inert materials. This configuration limits the efficient ignition of the coal embers, thus leading to excessive fuel consumption. For a hot start, the specific fuel consumptions decrease, with values of  $0.061 \pm 0.002$  kg/L for test 1 compared to  $0.098 \pm 0.002$  kg/L for test 2. This phase demonstrates good fuel economy for both tests, however, test 1 shows the best. The low value for test 2 could be due to unfavorable weather conditions, including moderate wind speed, low relative humidity, and low ambient temperature. The final phase, corresponding to simmering, shows a specific consumption of  $0.104 \pm 0.003$  kg/L for test 1, higher than that of test 2, estimated at  $0.062 \pm 0.002$  kg/L. During this phase, both tests show a slight consumption of charcoal, attributed to the thermal storage role played by the inert materials, promoting more stable temperature regulation in the firebox. **Figure 12** shows the boiling efficiency of charcoal plus inert material in a size 3 pot.

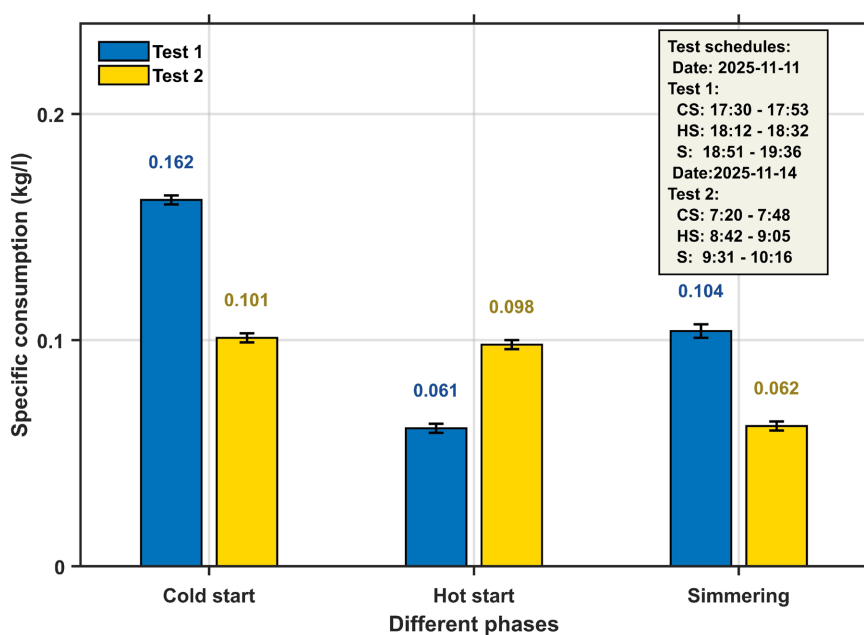


**Figure 11.** Comparison of the Specific Consumption of Charcoal, Wood Plus Inert Material in Two Trials of a Size 3 Pot.

**Figure 12** shows low efficiency during cold start-up. Indeed, test 2 is more efficient than test 1, with values of  $14.78 \pm 0.04\%$  for test 1 and  $17.7 \pm 0.09\%$  for test 2. This decrease in efficiency is explained by heat losses through convection between the firebox walls and the ambient air, as well as poor conduction between the coal embers and the bottom of the pot. During the hot start-up phase, the efficiency of test 1 is almost double that of test 2:  $40.69 \pm 0.26\%$  for test 1 versus  $20.66 \pm 0.09\%$  for test 2. This increase is due to better combustion in test 1, promoting direct heat transfer to the bottom of the pot. During the simmering phase, yields are relatively high, with  $31.94 \pm 0.12\%$  for trial 1 and  $48.49 \pm 0.25\%$  for trial 2. This improvement is due to good thermal convection between the heat source

and the pot. **Figure 13** shows the specific boiling time of charcoal mixed with inert materials in a size 3 pot.

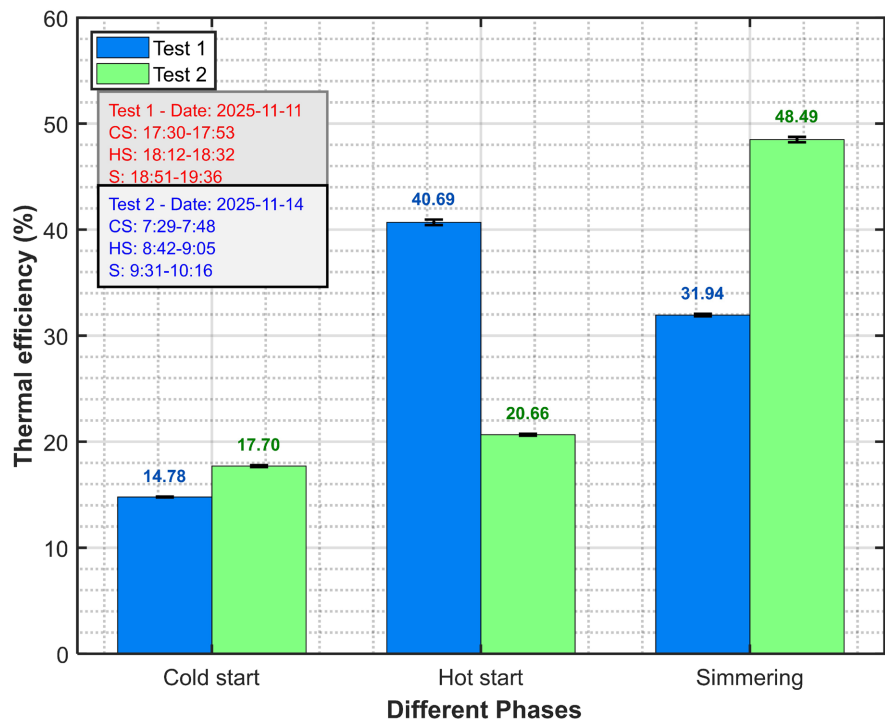


**Figure 12.** Boiling efficiency of charcoal plus inert material in a size 3 pot.

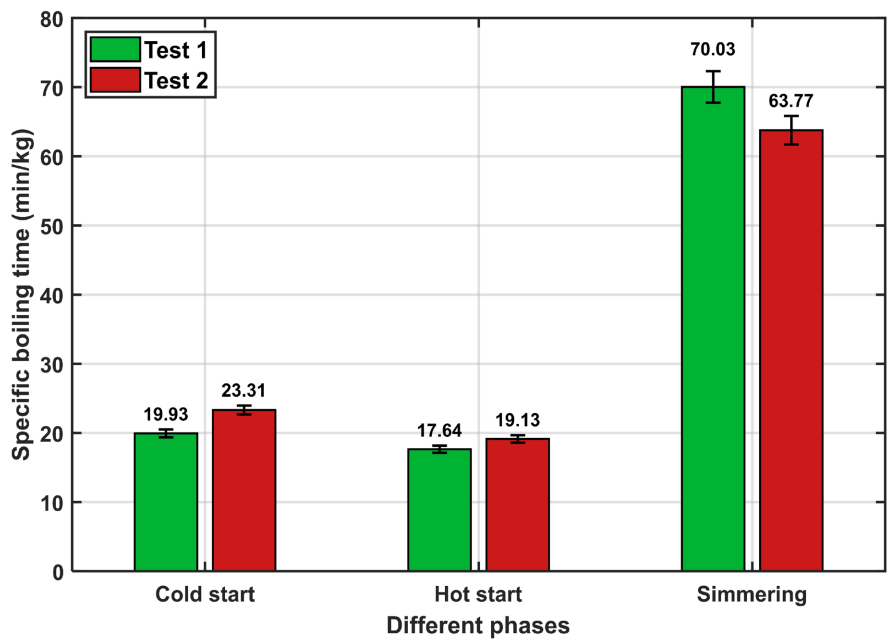


**Figure 13.** Specific boiling time of coal plus inert material in a size 3 pot.

**Figure 13** shows generally short specific boiling times during the two high-power phases, with a maximum boiling time of 24 min/L. During the cold start,

the values obtained were  $19.93 \pm 0.57$  min/L and  $23.31 \pm 0.65$  min/L for tests 1 and 2, respectively. Test 1 exhibits a shorter boiling time, indicating lower heat losses and better heat transfer to the bottom of the pot. During the hot start, the specific boiling time remains low, at  $17.64 \pm 0.52$  min/L for test 1 compared to  $19.13 \pm 0.53$  min/L for test 2. The short time observed for test 1 can be explained by more efficient heat conduction between the heat source and the cooking vessel. During the simmering phase, the values are relatively close, reaching  $70.03 \pm 2.75$  min/L for test 1 and  $63.77 \pm 2.06$  min/L for test 2. These values, exceeding 45 min/L, are explained by the imposed duration of this phase, set at 45 minutes. In general, test 1 exhibits lower specific consumption, which can be attributed to the presence of a greater quantity of inert materials promoting the accumulation and gradual release of heat. It also displays better thermal efficiencies during the last two phases, as well as shorter boiling times. Test 2, on the other hand, is characterized by relatively homogeneous specific consumption across the different phases, with a higher thermal efficiency during the simmering phase, but slightly longer boiling times than those of test 1.

### 3.2.2. Evolution of Thermal Efficiency as a Function of fire Power for the Size 3 Pot

**Figure 14** represents the thermal efficiency as a function of the fire power of the size 3 pot (coal plus inert material).

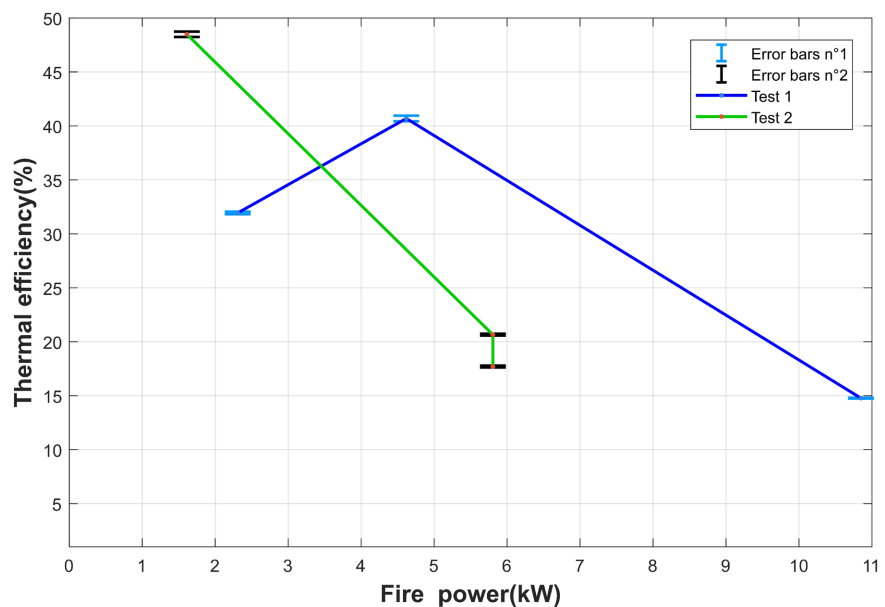


**Figure 14.** Thermal efficiency as a function of the fire power of a size 3 pot (charcoal plus inert material).

**Figure 14** shows a high-power output of 10.848 kW for test 1 and an average power output of 5.805 kW for test 2 at cold start, with respective efficiencies of  $14.78 \pm 0.04\%$  for test 1 and  $17.7 \pm 0.09\%$  for test 2. When the fire power is too high, the efficiency decreases. This is due to significant heat losses from convec-

tion with the ambient air and radiation through the firebox walls. At hot start, the power output of test 1 is 4.619 kW, while that of test 2 remains the same as the previous one (5.805 kW), with respective efficiencies of  $40.69 \pm 0.26\%$  and  $20.66 \pm 0.09\%$ . The high efficiency of test 1 is explained by better thermal contact between the coal embers and the pot, thus limiting heat loss. However, test 2 is characterized by less efficient combustion, probably due to less favorable thermal contact between the embers and the pot. During the simmering phase, the power outputs are relatively low: 2.309 kW for test 1 and 1.611 kW for test 2. Conversely, these efficiencies are highest during this phase:  $31.94 \pm 0.12\%$  for test 1 and  $48.49 \pm 0.25\%$  for test 2. These two high values are explained by good contact between the coal embers and the direct contact with the pot, which minimizes heat loss.

### 3.2.3. Evolution of Water Temperature over Time in a Size 3 Pot

Figure 15 shows the temporal evolution of the water in the size 3 pot.

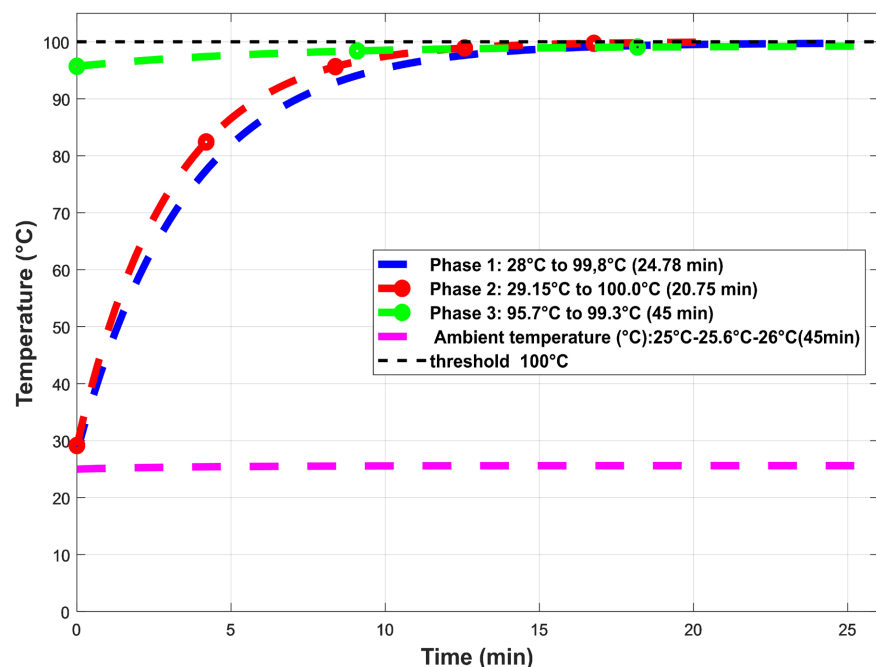


Figure 15. Evolution of water temperature over time in a size 3 pot.

Figure 15 shows the three phases of the TEE (Thermal Energy Evaluation) process and the relatively constant ambient air temperature throughout. Phase 1 reaches boiling point in 24.78 minutes, followed by Phase 2 in 20.75 minutes. This high-power output results in a moderately fast boiling time, leading to less heat loss to the environment with moderate thermal power. Indeed, the pot receives heat directly, which promotes rapid boiling. The simmering phase is quite long, maintaining the water temperature slightly below boiling. The ambient temperature curve remains almost constant over time. This is explained by the fact that the external environment did not undergo significant changes (no significant variation in wind, humidity, etc.).

### 3.3. Comparison of Results with Literature

The results obtained generally confirm the trends reported in the literature on improved biomass cookstoves. In particular, the measured thermal efficiencies ( $\approx 23\%$  to  $48\%$ ) fall within the typical range for improved cookstoves reported by Berrueta *et al.* (2008), who indicate efficiencies generally between  $20\%$  and  $40\%$  for optimized systems operating on wood or charcoal [20]. The high values observed during the simmering phase (up to  $48.49\%$ ) even exceed some conventional performances, which can be attributed to the thermal inertia effect of the integrated materials. The improved efficiency in the presence of inert materials is consistent with the work of Darlami *et al.* (2019) and Atajafari *et al.* (2024), which shows that the use of refractory or high-thermal-capacity materials helps stabilize the thermal regime and reduce energy losses [7] [9]. In our study, this improvement is particularly pronounced during the simmering phase, which aligns with the observations of Vitoussia *et al.* (2021) on the role of thermal storage in improved cookstoves [14]. In terms of specific consumption, the values obtained ( $\approx 0.061$  to  $0.143$  kg/L) are comparable to those reported by Kassahun and Alemu (2022), who demonstrate a significant reduction in biomass consumption thanks to improved technologies [11]. The decrease observed in your trials, particularly with pot #3, confirms that optimizing heat transfer (better contact between the cookstove and the pot) is a determining factor, as also highlighted by Amoah *et al.* (2021) [8]. Regarding the specific boiling time, your results show a notable improvement with pot 3 ( $\approx 17 - 24$  min/L), which is consistent with the findings of Okafor and Unachukwu (2012), according to whom a better geometric fit between the burner and the pot significantly reduces cooking times [18]. Furthermore, the reduction in boiling time when starting from a hot temperature is consistent with the observations of Bailis *et al.* (2007) within the WBT protocol [21].

Furthermore, the inverse relationship observed between fire power and thermal efficiency (lower efficiency at higher power) is well documented in the literature. De Lepeleire *et al.* (1983) explain this phenomenon by the increase in convection and radiation losses when the combustion intensity is high, which perfectly matches the trends observed in your results [2]. Finally, the influence of pot size on performance confirms the conclusions of several studies (notably Amou *et al.* (2018)), which show that geometric suitability improves heat transfer and limits losses [19]. In our case, the superiority of pot 3 clearly validates this principle.

### 4. Conclusion

This study, which follows on from our work on the influence of pot size on the thermo-energy performance of improved cookstoves, allowed us to evaluate the effect of integrating inert materials (quartz) into a charcoal-fired cookstove. The experimental results obtained using the Water Boiling Test (WBT) protocol clearly show that the presence of these materials improves heat flow management and the energy stability of the system. For the size 2 pot, test 1 proved to be the most fuel-efficient, with a minimum specific consumption of  $0.069 \pm 0.003$  kg/L at cold start,

compared to  $0.072 \pm 0.003$  kg/L for test 2. During the simmering phase, the thermal efficiency of test 1 reached  $38.38 \pm 0.33\%$ , while that of test 2 fell to  $12.7 \pm 0.13\%$ , reflecting better heat release by the inert materials in the first case. In contrast, test 2 exhibited faster heating, with a specific boiling time of  $23.71 \pm 0.67$  min/L at the hot start, compared to  $28.45 \pm 0.79$  min/L for test 1. Regarding the size 3 pot, the overall performance appears more promising. The best thermal efficiency was observed at the hot start in test 1, with a value of  $40.69 \pm 0.26\%$ , while the simmering phase of test 2 reached  $48.49 \pm 0.25\%$ , the highest value in the entire study. The specific boiling times were also lower than those of pot 2, with  $17.64 \pm 0.51$  min/L and  $19.13 \pm 0.53$  min/L for tests 1 and 2, respectively, at the hot start. Furthermore, the specific consumption drops to  $0.061 \pm 0.002$  kg/L, confirming excellent fuel economy. The comparative analysis shows that pot 3 offers the best geometric fit with the firebox, promoting better thermal contact between the embers, inert materials, and the bottom of the pot. This configuration allows for the development of suitable power outputs, ranging from 1.611 kW to 10.848 kW, with efficiencies exceeding 48%. Ultimately, the integration of quartz into the firebox significantly improves thermo-energy performance by promoting the storage and gradual release of heat, particularly during simmering phases. Among the tested configurations, the size 3 pot, combined with charcoal and inert materials, is the most efficient solution, combining low specific consumption, high efficiency, and reduced boiling time. These results open up interesting possibilities for the optimal sizing of improved, high-energy-efficiency domestic stoves.

### Conflicts of Interest

The authors declare no conflicts of interest regarding the publication of this paper.

### References

- [1] Bailis, R., Berrueta, V., Chengappa, C., Dutta, K., Edwards, R., Masera, O., *et al.* (2007) Performance Testing for Monitoring Improved Biomass Stove Interventions: Experiences of the Household Energy and Health Project. *Energy for Sustainable Development*, **11**, 57-70. [https://doi.org/10.1016/s0973-0826\(08\)60400-7](https://doi.org/10.1016/s0973-0826(08)60400-7)
- [2] De Lepeleire, G. and Christiaens, M. (1983) Heat Transfer and Cooking Woodstove Modelling. *Proceedings of the Indian Academy of Sciences Section C: Engineering Sciences*, **6**, 35-46. <https://doi.org/10.1007/bf02843289>
- [3] Honkalaskar, V.H., Bhandarkar, U.V. and Sohoni, M. (2013) Development of a Fuel Efficient Cookstove through a Participatory Bottom-Up Approach. *Energy, Sustainability and Society*, **3**, Article No. 16. <https://doi.org/10.1186/2192-0567-3-16>
- [4] Prasad, K.U., Iqbal, M.A. and Urry, D.W. (1985) Utilization of 1-Hydroxybenzotriazole in Mixed Anhydride Coupling Reactions. *International Journal of Peptide and Protein Research*, **25**, 408-413. <https://doi.org/10.1111/j.1399-3011.1985.tb02193.x>
- [5] Randhawa, G. and Arora, S. (2016) An Insight into Conceptualization of Quality of Work Life. *Pacific Business Review International*, **8**, 93-99.
- [6] Kassahun, T. and Alemu, D. (2022) Thermal Efficiency Improvement of Biomass Cookstoves. *Case Studies in Thermal Engineering*, **3**, 19-36.
- [7] Darlami, H.B., Ale, B.B. and Pokharel, G.R. (2020) Experimental Analysis of Thermal

- Efficiency of Mud Improved Cookstove with Variation of Different Parameters and Economic Analysis. *Journal of the Institute of Engineering*, **15**, 385-392. <https://doi.org/10.3126/jie.v15i3.32228>
- [8] Obeng, G.Y., Mensah, E. and Opoku, R. (2021) Fabricators and End-Users of Single-Pot Biomass Stoves: Conceptualizing, Hypothesis and Performance Metrics for Developing Energy Sustainability Framework. *Sustainability*, **13**, Article 7098. <https://doi.org/10.3390/su13137098>
- [9] Atajafari, H., Pathak, B.R. and Bhandari, R. (2024) Thermal Performance Evaluation of a Single-Mouth Improved Cookstove: Theoretical Approach Compared with Experimental Data. *Energies*, **17**, Article 4355. <https://doi.org/10.3390/en17174355>
- [10] Ouedraogo, D., Sawadogo, G.L., Kabore, B., Sana, A. and Igo, S.W. (2026) Experimental Assessment of the Thermal Efficiency of an Improved Biomass Cookstove Fueled by Charcoal and Wood: Influence of Cooking Pot Size under Water Boiling Test Conditions. *International Journal of Environment and Climate Change*, **16**, 111-123. <https://doi.org/10.9734/ijecc/2026/v16i55425>
- [11] Mekonnen, B.A. (2022) Thermal Efficiency Improvement and Emission Reduction Potential by Adopting Improved Biomass Cookstoves for Sauce-Cooking Process in Rural Ethiopia. *Case Studies in Thermal Engineering*, **38**, Article ID: 102315. <https://doi.org/10.1016/j.csite.2022.102315>
- [12] Deng, M., Zhang, P., Yang, H. and Ma, R. (2023) Directions to Improve the Thermal Efficiency of Household Biomass Cookstoves: A Review. *Energy and Buildings*, **278**, Article ID: 112625. <https://doi.org/10.1016/j.enbuild.2022.112625>
- [13] Modi, B., Timilsina, H., Bhandari, S., Achhami, A., Pakka, S., Shrestha, P., *et al.* (2021) Current Trends of Food Analysis, Safety, and Packaging. *International Journal of Food Science*, **2021**, 1-20. <https://doi.org/10.1155/2021/9924667>
- [14] Vitoussia, T., Brillard, A., Bertsch, J., Allgaier, O., Leyssens, G., Schönnenbeck, C., *et al.* (2021) Analysis and Modeling of the Thermal Behavior of an Improved Pellet Cookstove. *SN Applied Sciences*, **3**, Article No. 652. <https://doi.org/10.1007/s42452-021-04630-4>
- [15] Destaw, F., Birhanu, A. and Gurmessa, A. (2025) Performance Evaluation of Improved Biomass Cookstoves Used in Gambella Refugee Camps, Southwest Ethiopia. *Discover Energy*, **5**, Article No. 39. <https://doi.org/10.1007/s43937-025-00101-8>
- [16] Tanoh, T.S., Kpai, N.N., Sidibe, S.D.S. and Sawadogo, M. (2017) Étude de l'influence de la taille de la marmite sur l'efficacité énergétique d'un foyer amélioré de type ménage. *Afrique SCIENCE*, **13**, 284-291.
- [17] Boureima, D., Adélaïde, O.L., Abdoulaye, C., Estelle, Z.W., Sié, K. and Bathiébo, D.J. (2024) Experimental Study of Improved Cookstove with Primary and Secondary Sources. *World Journal of Advanced Research and Reviews*, **23**, 907-917. <https://doi.org/10.30574/wjarr.2024.23.1.2058>
- [18] Muralidharan, V., Sussan, T., Limaye, S., Koehler, K., Williams, D., Rule, A., *et al.* (2015) Field Testing of Alternative Cookstove Performance in a Rural Setting of Western India. *International Journal of Environmental Research and Public Health*, **12**, 1773-1787. <https://doi.org/10.3390/ijerph120201773>
- [19] Okafor, I.F. and Unachukwu, G.O. (2012) Performance Evaluation of Nozzle Type Improved Wood Cook Stove. *American-Eurasian Journal of Sustainable Agriculture*, **6**, 195-203.
- [20] Amou, K.A., Sagna, K., N'witicha, K., Saa, T. and Napo, K. (2018) Study and Design of an Improved Clay Conical Stove. *International Journal of Recent Scientific Research*,

- 9, 29909-29915.
- [21] Berrueta, V.M., Edwards, R.D. and Masera, O.R. (2008) Energy Performance of Wood-Burning Cookstoves in Michoacan, Mexico. *Renewable Energy*, **33**, 859-870. <https://doi.org/10.1016/j.renene.2007.04.016>
- [22] Bailis, R., Ogle, D., MacCarty, N., Smith, K.R. and Edwards, R. (2007) The Water Boiling Test (WBT). 38 p. [https://energypedia.info/images/3/38/Wbt\\_version\\_3.0\\_jan2007.pdf](https://energypedia.info/images/3/38/Wbt_version_3.0_jan2007.pdf)
- [23] Jetter, J., Zhao, Y., Smith, K.R., Khan, B., Yelverton, T., DeCarlo, P., *et al.* (2012) Pollutant Emissions and Energy Efficiency under Controlled Conditions for Household Biomass Cookstoves and Implications for Metrics Useful in Setting International Test Standards. *Environmental Science & Technology*, **46**, 10827-10834. <https://doi.org/10.1021/es301693f>
- [24] Kshirsagar, M.P. and Kalamkar, V.R. (2014) A Comprehensive Review on Biomass Cookstoves and a Systematic Approach for Modern Cookstove Design. *Renewable and Sustainable Energy Reviews*, **30**, 580-603. <https://doi.org/10.1016/j.rser.2013.10.039>
- [25] Mekonnen, B.A., Ambushe, A.A. and Addisu, A. (2022) Performance Evaluation of Improved Biomass Cookstoves: A Review on Efficiency and Emission Reduction. *Energy for Sustainable Development*, **69**, 1-12.

## Abbreviations and Acronyms

$TES$	Specific boiling time (min/L)
$TEB$	Time taken to bring to a boil (min)
$M_s$	Mass of the pot filled with a standard quantity of water (kg)
$M_{es}$	Total mass (pot, lid, thermometer and stand (kg)
$T_i$	Initial water temperature (°C)
$\eta_{abl}$	boiling point thermal efficiency (%)
$C_{pe}$	Specific heat capacity of water (in 4186 kJ/kg.°C)
$T_{abl}$	Boiling's temperature (°C)
$M_i$	Initial mass of water (kg)
$T_i$	Initial water temperature (°C)
$L_v$	Latent heat of vaporization of water (2257 kJ/k)
$M_{ev}^{abl}$	Mass of water evaporated during the boiling test (in kg)
$PCI$	Lower heating value of coal: 29,000 kJ/kg
$M_b^{abl}$	Mass of wood consumed during the boiling test (kg)
$CS$	Specific coal consumption (kg/L)
$M_{cons}$	Mass of coal consumed (kg)
$M_{res}$	Mass of water remaining after each phase (kg)
$P$	The power of fire (W)
$M_{cons}$	The mass of fuel consumed for each phase (kg)
$PCI$	Lower Calorific Value (KJ/kg)
$t_f$	Final time (min)
$t_i$	Initial time (min)
$\tau_c$	combustion rate (g/min)
$M_{cons}$	mass of coal consumed for each phase of the test (kg)